

Hypoxic preconditioning protects rat hearts against ischaemia–reperfusion injury: role of erythropoietin on progenitor cell mobilization

Jih-Shyong Lin¹, Yih-Sharng Chen², Han-Sun Chiang³ and Ming-Chieh Ma³

¹Department of Medical Research, Tao-Yuan General Hospital, Taoyuan, Taiwan

²Department of Cardiovascular Surgery, National Taiwan University Hospital, Taipei, Taiwan

³School of Medicine, Fu Jen Catholic University, Hsinchuang, Taiwan

Preconditioning, such as by brief hypoxic exposure, has been shown to protect hearts against severe ischaemia. Here we hypothesized that hypoxic preconditioning (HPC) protects injured hearts by mobilizing the circulating progenitor cells. Ischaemia–reperfusion (IR) injury was induced by left coronary ligation and release in rats kept in room air or preconditioned with 10% oxygen for 6 weeks. To study the role of erythropoietin (EPO), another HPC + IR group was given an EPO receptor (EPOR) antibody via a subcutaneous mini-osmotic pump 3 weeks before IR induction. HPC alone gradually increased haematocrit, cardiac and plasma EPO, and cardiac vascular endothelial growth factor (VEGF) only in the first two weeks. HPC improved heart contractility, reduced ischaemic injury, and maintained EPO and EPOR levels in the infarct tissues of IR hearts, but had no significant effect on VEGF. Interestingly, the number of CD34⁺CXCR4⁺ cells in the peripheral blood and their expression in HPC-treated hearts was higher than in control. Preconditioning up-regulated cardiac expression of stromal derived factor-1 (SDF-1) and prevented its IR-induced reduction. The EPOR antibody abolished HPC-mediated functional recovery, and reduced SDF-1, CXCR4 and CD34 expression in IR hearts, as well as the number of CD34⁺CXCR4⁺ cells in blood. The specificity of neutralizing antibody was confirmed in an H9c2 culture system. In conclusion, exposure of rats to moderate hypoxia leads to an increase in progenitor cells in the heart and circulation. This effect is dependent on EPO, which induces cell homing by increased SDF-1/CXCR4 and reduces the heart susceptibility to IR injury.

(Received 4 August 2008; accepted after revision 8 October 2008; first published online 9 October 2008)

Corresponding author M.-C. Ma: School of Medicine, Fu Jen Catholic University, 510 Chungcheng Road, Hsinchuang 242, Taiwan. Email: med0041@mail.fju.edu.tw

Effective cardioprotection against ischaemia–reperfusion (IR) injury is one of the most important goals of experimental and clinical research in cardiology. The increased survival of cardiomyocytes subjected to IR injury can be achieved by prior repeated exposure to sublethal ischaemia or hypoxia, a phenomenon known as preconditioning (Murry *et al.* 1986; Cai *et al.* 2003). The first description of the protective effect of hypoxic preconditioning (HPC) was in the heart (Bernhardt *et al.* 2007), and the effects of HPC on the tissues of experimental animals depend on the protocol of hypoxic exposure used (Clanton & Klawitter, 2001; Neubauer, 2001). However, adapting whole animals to chronic intermittent hypoxia as an HPC has been shown to increase cardiac tolerance to the major deleterious

consequences of myocardial infarction caused by acute oxygen deprivation (Kolár & Ostádal, 2004; Lachmanova *et al.* 2005; Kolár *et al.* 2007). Several processes are known or believed to be involved in HPC-mediated tissue protection; these include oxygen transport, energy metabolism, neurohumoral regulation, redox balance, stress protein and protein kinase signalling, adenosine release, ATP-sensitive potassium channels, mitochondrial function, control of calcium levels, and nitric oxide production (Das & Maulik, 2006). However, the detailed mechanism(s) underlying HPC remain to be elucidated; in particular, the role of progenitor cells in this phenomenon remains unknown.

Stem cell therapy has exciting potential in organ protection, since the plasticity of progenitor cells may allow them to positively remodel and/or regenerate viable organ tissues, including those of the heart (Kucia *et al.*

J. S. Lin and Y. S. Chen contributed equally to this work.

2005a). Among the various stem cells, haematopoietic stem cells (HSCs) have shown particular promise for conferring protection on and repair of damaged tissue; however, studies researching the engraftment or transdifferentiation of HSCs have led to controversy concerning the mechanism(s) behind these promising effects (Murry *et al.* 2004; Balsam *et al.* 2004). An alternative approach is to manipulate the natural factors responsible for the homing of bone marrow-derived non-HSCs to the sites of injury (Kucia *et al.* 2005a,b). After myocardial IR, circulating bone marrow-derived cells can be detected in the peri-infarct region as endothelial cells and myocytes; this strongly suggests the presence of local chemotactic factors to guide cell homing to the injured heart (Jackson *et al.* 2001; Murry *et al.* 2004).

Studies have shown that erythropoietin (EPO) not only regulate erythropoiesis but activates a number of signalling kinases in rescuing cardiomyocytes directly and also modulates a host of cellular processes in pluripotent stem cell development and angiogenesis in response to cardiac injury (Maiese *et al.* 2005). In the rat model of chronic heart failure, EPO treatment improved cardiac function, and induced neovascularization requires the enhanced expression of vascular endothelial growth factor (VEGF) and the mobilization of the endothelial progenitor cells (Westenbrink *et al.* 2007). Specific cardiac VEGF induction in transgenic mice results in recruitment and retention of bone marrow-derived circulating cells in close proximity to angiogenic vessels, which is mediated by stromal derived factor-1 (SDF-1) (Grunewald *et al.* 2006). The overexpression of SDF-1 by vector transfection or its early up-regulation in IR hearts has been shown to improve ventricular function, suggesting that SDF-1 is an essential factor for mobilizing stem cells (Askari *et al.* 2003; Tang *et al.* 2005). Moreover, use of an antagonist against the SDF-1 receptor CXCR4 to block the SDF-1/CXCR4 interaction reduces cell homing to the infarct heart (Abbott *et al.* 2004). An SDF-1 concentration gradient across the tissue appears to be the major mechanism for stem cell homing to the damaged heart.

Here we test the hypothesis in a rat model of acute myocardial infarction that if the cardiac concentration gradient of SDF-1 or VEGF were increased by HPC via EPO signalling, which is known to be involved in cardioprotection (Cai *et al.* 2003; Parsa *et al.* 2003; Maiese *et al.* 2005; Chan *et al.* 2007), CD34⁺CXCR4⁺ cells would home to the heart and thereby improve function of the postischaemic heart.

Methods

Animals

Female Wistar rats, weighing 200–220 g, were used. All animal experiments and care were performed in

accordance with the *Guide for the Care and Use of Laboratory Animals* (National Research Council, 1996). The Laboratory Animal Care Committee of Fu Jen Catholic University approved all protocols in this study.

Induction of HPC

HPC was induced by maintaining rats in a chamber constantly flushed with nitrogen to reduce the oxygen content to 10% (Biospherix, Redfield, NY, USA) for 8 h per day (09.00–17.00 h) and then returning to room air after hypoxic induction, as previously described (Milano *et al.* 2002). The induction time is 6 weeks. The haematocrit was measured every week from tail vein blood collected in heparinized capillary tubes.

Induction of acute myocardial infarction

The rats were anaesthetized by intraperitoneal ketamine (60 mg kg⁻¹) and sodium pentobarbital (35 mg kg⁻¹). The rats were ventilated with room air at 60 breaths min⁻¹ and a tidal volume of 8 ml kg⁻¹ after intubation. The rectal temperature was maintained at 37°C with a servo-null heating pad. Left thoracotomy was performed under aseptic conditions. The left anterior descending artery close to its origin, about 3 mm away from the left coronary ostium, was looped with 7-O Prolene (Ethicon Inc., Somerville, NJ, USA), as previously described (Chen *et al.* 2005). The looped stitch was snared for 40 min, and then released. Ischaemia was confirmed by the appearance of regional cyanosis on the epicardium distal to the ligation, or by akinesia or bulging in this area. After ischaemia, the thorax was closed under aseptic conditions and each rat was returned to its own cage for recovery for 3 days.

Preparation of isolated perfused hearts

Rats were anaesthetized with sodium pentobarbital (50 mg kg⁻¹, i.p.), and blood was collected from the abdominal aorta into a heparinized tube for further analyses of cardiac enzymes, cell numbers and EPO content. One millilitre of 500 IU heparin was immediately given via the inferior vena cava. The hearts were rapidly excised, weighed, and immersed in ice-cold Krebs–Henseleit buffer, as previously described (Chan *et al.* 2007). After a 30 min non-circulating perfusion to remove the blood cells, the following were recorded continuously and averaged for 20 min: the coronary perfusion pressure at the aorta, the left ventricular developed pressure (LVDP) measured by inserting a water-filled latex balloon, and the heart rate (transformed from the LVDP curve).

Measurement of infarction

At the end of perfusion, the heart was weighed and sliced. A middle slice was used to evaluate infarction, as previously described (Chan *et al.* 2007). The slice was incubated for 20 min at 37°C in a 1% 2,3,5-triphenyltertrazolium chloride (Sigma) solution to distinguish between the infarct (pale) and viable (red) regions. Then, the tissues from infarct area or the corresponding area in the left ventricle were prepared for immunolabelling or stored at -80°C.

Creatine kinase-MB assay

The blood was centrifuged at 620 g and the plasma was collected to measure the activity of creatine kinase-MB (CK-MB) in an electrolyte analyser, as previously described (Chan *et al.* 2007).

ELISA for EPO and VEGF

Quantitative immunoassays were used to determine the level of EPO (Biomerica, Newport Beach, CA, USA) and VEGF (Quantikine M murine, R&D Systems, Minneapolis, MN, USA) in accordance with the manufacturer's protocol. The total protein in the blood and in the homogenized tissue extracts was quantified by a commercial kit (Bio-Rad, Hercules, CA, USA).

Detection of CD34⁺ or CXCR4⁺ cells in peripheral blood

Peripheral blood (1 ml) was centrifuged at 1200 g with a 40% Ficoll solution to collect the white blood cells on the top layer. After washing twice with phosphate-buffered saline (PBS; pH 7.4), the cells were postfixed with 100 μ l of 4% formaldehyde in PBS at room temperature (RT) for 20 min. The cells were then incubated with phycoerythrin-conjugated anti-CD34 (1 : 50 dilution, BD Biosciences, Franklin Lakes, NJ, USA) and rabbit anti-CXCR4 (1 : 200 dilution, Santa Cruz Biotechnology, Santa Cruz, CA, USA) at RT for 1 h. Unbound antibodies were washed twice with PBS, and CXCR4 was further detected by a tyramide signal amplification (TSA) kit after incubation with HRP-conjugated anti-rabbit IgG (1 : 500 dilution, Jackson ImmunoResearch, West Grove, PA, USA), according to the manufacturer's instructions (NEN Life Science, Boston, MA, USA). Nuclei were then counterstained with DAPI. Fluorescence was examined with an Olympus BX51 microscope (Tokyo, Japan) equipped with a fluorescence image analytic system (Diagnostic Instruments, Sterling Heights, MI, USA). The total leukocyte count was further examined by Türk's solution.

In vitro study for EPOR antibody

H9c2 (2-1) cells (CRL-1446) were obtained from the American Type Culture Collection (ATCC, Rockville, MD, USA) and cultured in Dulbecco's modified Eagle's medium (Biosera, Barcelona, Spain) supplemented with 10% (v/v) fetal bovine serum (Thermo Fisher Scientific, MA, USA). Cells were plated at a density of about 0.6×10^4 cells cm^{-2} in 35 mm dishes and were grown under 5% CO₂ in a water-saturated incubator (NuAire, Plymouth, MN, USA) as previously described (Parsa *et al.* 2003).

Control cells were fixed with freshly prepared 3% paraformaldehyde in PBS for 10 min at 4°C. After they were washed with PBS, the cells were permeabilized in PBS containing 0.5% Triton X-100 for 3 min and blocked in 3% bovine serum albumin (BSA). The cells were incubated overnight at 4°C with rabbit polyclonal antibody against EPO receptor (EPOR) (sc-697, Santa Cruz) diluted in 3% BSA and then incubated with rhodamine-Red-X-conjugated IgG at RT for 1 h. Nuclei were counterstained with DAPI. The cells were mounted with antifading solution and examined with a fluorescence microscope as above. Negative staining was performed by preadsorption of EPOR antibody with blocking peptide (Santa Cruz).

To confirm the specificity of EPOR antibody used *in vivo*, cells were treated with 5 U ml^{-1} of EPO or combinations of EPO (5 U ml^{-1}) and EPOR antibody at 5, 10, or 30 ng ml^{-1} for 1 h at 37°C. Culture medium was collected for lactate dehydrogenase (LDH) assay and the cells were harvested for Western blot as previously described (Ma *et al.* 2005).

Preparation of the mini-osmotic antibody-releasing pump

The mini-osmotic pump (model 2004; Alzet, CA, USA) was placed into a saline bath at 37°C for 4 h before being implanted subcutaneously into the rat, according to the manufacturer's instruction. The pump was carefully filled with EPOR antibody (same as above) solution (200 μ l) at concentration of 0.2 $\mu\text{g} \mu\text{l}^{-1}$ by using a Hamilton syringe so as to avoid gas residue in the pump. The total amount of antibody would be released in 28 days at a rate of 0.6 μg per day. All procedures were implemented under sterile conditions. The pump was filled with the same volume of normal rabbit IgG (sc-2027, Santa Cruz) for the control group.

RT-PCR for quantification of CD34 and CXCR4 expressions

The heart samples were taken from the left ventricles in groups. More specifically, tissue containing infarct

area was sampled in IR and HPC + IR hearts, but only the corresponding area in control and HPC hearts was taken. RNA was isolated with a Trizol kit (Invitrogen), as previously described (Ma *et al.* 2005). Briefly, cDNA was synthesized at 42°C for 45 min using 5 µg each of total RNA and poly(dT)₁₅ oligonucleotide primer (Invitrogen) and 200 units of reverse transcriptase (Moloney murine leukaemia virus; Promega, Madison, WI, USA). CD34 (XM223083) primers were as follows: forward, 5'-AGT CCC AA GGA GAA AGG CTG-3' and reverse, 5'-TCA CAG TTC TGT GTC AGC CAC-3'. The primer sequences for CXCR4 (U90610) were forward, 5'-ATG GGT TGG TAA TCC TGG TC-3' and reverse, 5'-TGA TGA AGG CCA GGA TGA GA-3', and those for glyceraldehyde-3-phosphate dehydrogenase (GAPDH, XR007956) were 5'-TTA GCA CCC CTG GCC AAG G-3' and 5'-CTT ACT CCT TGG AGG CCA TG-3'. PCR began with a 1 min, 94°C denaturation step followed by 40, 35, and 30 cycles for CD34, CXCR4 and GAPDH, respectively, at 94°C for 30 s, 58°C for 1 min, and 72°C for 1 min. The PCR products were electrophoresed through a 2% agarose gel and visualized by ethidium bromide staining. The densities of the bands were measured using an image analytic system (Diagnostic Instruments) and the mRNA levels were expressed as the ratio of CXCR4 or CD34 to GAPDH.

Immunostaining for detection of protein expression

Western blot was performed as previously described (Chan *et al.* 2007; Feng *et al.* 2008). In brief, total protein of tissue or cell extract was prepared using a commercial extraction kit (BioVision, Mountain View, CA, USA) and was subjected to electrophoresis. Blotting was performed on rabbit antibody against EPOR (Santa Cruz; 1:1000 dilution) and mouse antibodies against SDF-1 (1:2000 dilution; Santa Cruz) or actin (Biomedica, Plovdiv, Bulgaria; 1:2000 dilution). Activation of Akt and ERK was assessed by using rabbit antibodies (Santa Cruz) raised against phosphorylated and total protein (all at 1:2500 dilution). After washing, the membrane was incubated with HRP-conjugated anti-mouse or anti-rabbit IgG antibody (Vector Laboratories Inc., Burlingame, CA, USA) and the bound antibody was visualized using a commercial ECL kit (Amersham Bioscience) and Kodak film. The densities of the bands for EPOR, SDF-1, actin, pAkt, Akt, pERK and ERK with respective molecular masses of 78, 10, 40, 70, 62, 44/42 and 44/42 kDa were determined using an image analysing system (Diagnostic Instruments).

Tissue slices were frozen in Optimal Cutting Temperature (O.C.T.) compound and SDF-1 expression was detected by indirect immunofluorescent staining, as previously described (Feng *et al.* 2008). Briefly, 5 µm sections were fixed in 4% formaldehyde. After blocking

endogenous peroxidase, the goat anti- α -actinin antibody (1:1000 dilution; Santa Cruz) was added and incubated at RT for 1 h. FITC-conjugated rabbit anti-goat IgG (Jackson ImmunoResearch) was applied for 1 h. After visualization of α -actinin signal, the same section was further incubated with an anti-SDF-1 antibody (1:500 dilution; Santa Cruz) overnight. Rabbit anti-mouse or anti-goat IgG served as negative controls (Jackson ImmunoResearch). The next day, HRP-conjugated goat anti-mouse IgG was applied for 1 h at RT, and the slides were developed with TSA kit. Nuclei were counterstained with DAPI.

Statistical analysis

Numerical data are presented as means \pm S.E.M. Differences between groups were analysed using Student's unpaired *t* test or one-way ANOVA, with a *post hoc* test using Duncan's multiple-range test. Differences were regarded as significant for $P < 0.05$.

Results

Effects of HPC on EPO

Rats adapted well to 10% oxygen, with no mortalities. The weight gain in rats after 6 weeks of HPC was similar to that of control rats ($n = 16$ for each group). HPC gradually increased haematocrit levels in rats, with significant increases observed after 2 weeks of HPC, and with a plateau after 4–6 weeks (Fig. 1A). HPC also increased the plasma and cardiac content of EPO (Fig. 1B and upper panel in Fig. 1C), which remained significantly elevated at all time points except at week 3 for plasma EPO. However, the cardiac VEGF content was only significantly elevated at the first 2 weeks after HPC induction (lower panel in Fig. 1C).

HPC improves contractile function and reduces cardiac damage by IR

The LVDP was attenuated in IR hearts, which was associated with significant increases in infarct size and plasma CK-MB levels (Fig. 2). HPC exhibited no effect on these parameters in non-IR hearts, but largely improved LVDP and significantly reduced infarction and CK-MB release in IR hearts.

Changes in EPO and receptor expression after HPC and IR

IR had no significant effect on the plasma EPO levels (upper panel) but reduced the intracardial EPO content (middle panel); this was associated with an increase in intracardial VEGF content (lower panel) (Fig. 3A). HPC

markedly increased EPO levels in both cardiac tissue and plasma, but not cardiac VEGF. Interestingly, IR augmented the increased EPO level in plasma but did not significantly affect the levels of EPO and VEGF seen in the HPC-treated hearts.

We then examined the expression of EPOR in groups, which is also expressed on non-hematopoietic cells such as cardiomyocytes (Jones *et al.* 1990). HPC did not affect EPOR expression compared to control, but it prevented the IR-mediated EPOR reduction (Fig. 3B).

HPC increases CD34⁺ and CXCR4⁺ cells in peripheral blood and hearts

In control blood, the expression of CD34 and CXCR4 in peripheral nuclear cells was largely colocalized (Fig. 4A). CD34 and CXCR4 expression and the degree

of colocalization were increased in HPC compared to control blood. Of the 1×10^5 cells examined, the number of CD34⁺ or CXCR4⁺ cells in the HPC blood was 248.7 ± 22.1 and 184.4 ± 18.5 , respectively; both of these values were significantly higher than those in the control blood, which were 134.6 ± 16.5 and 96.4 ± 10.1 cells, respectively ($n = 4$). However, the total leukocyte count was similar between the control and HPC blood (14.8 ± 2.8 versus $14.3 \pm 2.7 \times 10^9$ per litre, respectively; $n = 4$).

CXCR4 mRNA, but not CD34 mRNA, was detected in control hearts (Fig. 4B). Interestingly, HPC markedly up-regulated both CXCR4 and CD34 mRNAs; this suggests that HPC mobilized CD34-expressing cells with CXCR4. CXCR4 mRNA levels were reduced in IR hearts, which was associated with increased CD34 mRNA levels

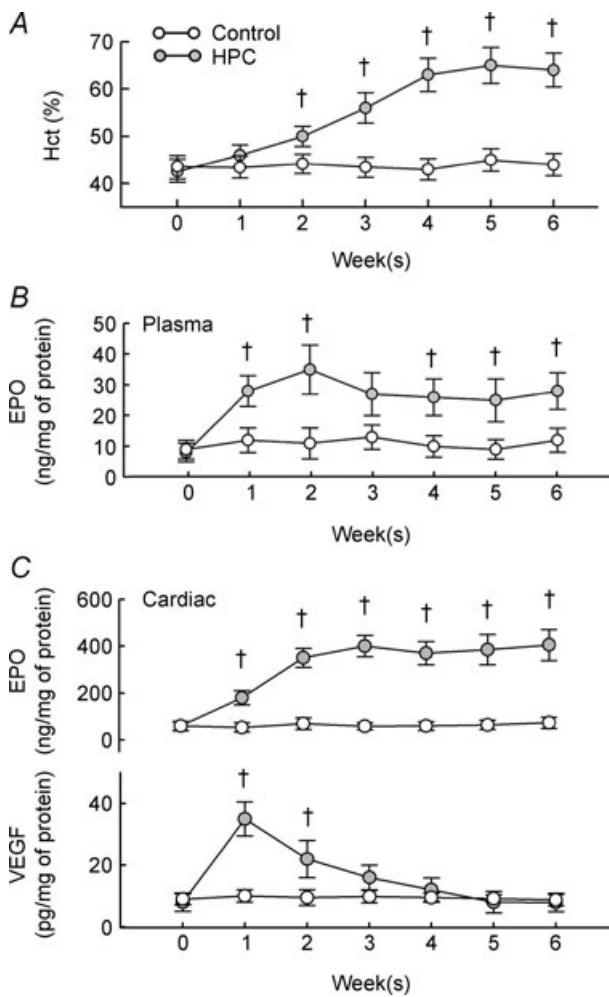


Figure 1. Effects of HPC
 A, changes in haematocrit (Hct) in control and HPC rats. $N = 16$ for each group. B and C, changes in the plasma levels of EPO (B) and intracardial levels of EPO and VEGF (C) after HPC. † $P < 0.05$ compared to the control group at the same week.

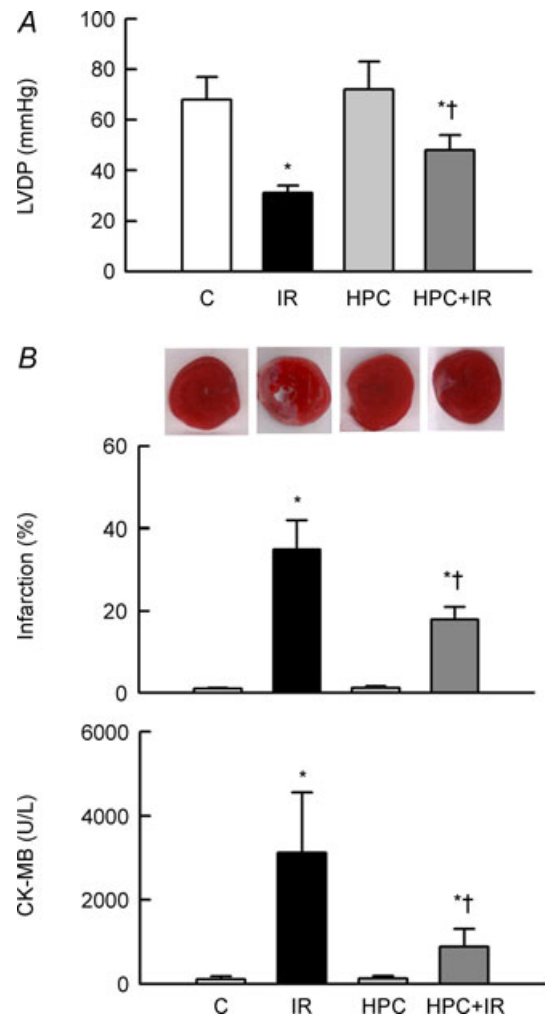


Figure 2. HPC ameliorates functional impairment and cardiac injury after IR
 A, changes in LVDP in groups. B, the degree of infarction (middle) with representative TTC-stained sections (upper), and release of the cardiac enzyme CK-MB (lower). * $P < 0.05$ compared to the control (C) group. † $P < 0.05$ compared to the IR group.

compared with control. However, HPC treatment of IR hearts restored the level of CXCR4 mRNA, and increased CD34 mRNA to a level similar to that in HPC hearts.

HPC increases SDF-1 expression in heart

The cardiac level of SDF-1 was significantly increased compared to control heart after IR or HPC, by

86.2 ± 15.7% and 202.6 ± 47.2%, respectively (Fig. 5A). Although the SDF-1 expression was low in the HPC + IR compared to HPC hearts, its expression remained > 2.1-fold elevated over control hearts ($P < 0.05$). Immunofluorescent staining showed that SDF-1 was expressed in the plasmalemma of cardiomyocytes with a lesser intracellular distribution in control hearts, but its expression was greatly increased and more widely distributed in HPC hearts (Fig. 5B).

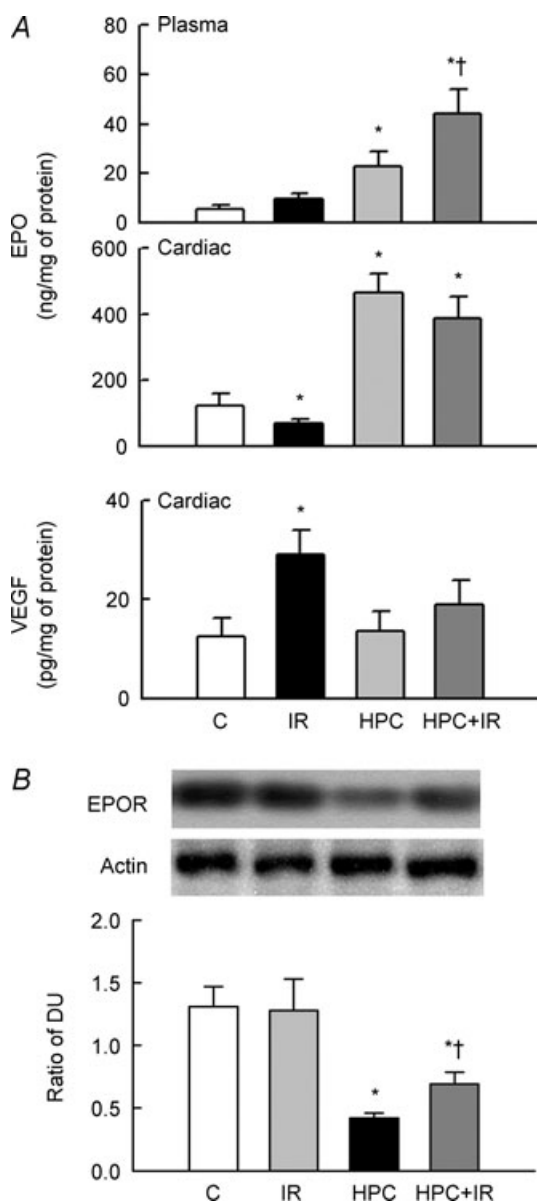


Figure 3. HPC increases EPO and prevents EPO receptor (EPOR) down-regulation

A, changes in EPO and VEGF levels in plasma or cardiac tissue ($n = 12$ in each group). Note that HPC increased EPO in both heart and plasma but not VEGF. B, the upper panel shows the representative blots for EPOR and actin expression. The lower bar graph shows the ratio of the density units (DU) of EPOR and actin ($n = 6$ in each group). * $P < 0.05$ compared to the control (C) group. † $P < 0.05$ compared to the IR group.

Antibody inhibits EPO signalling in H9c2 cardiomyoblasts

Figure 6A shows that EPOR was homogeneously expressed in H9c2 cells. Pre-adsorption of EPOR antibody (EPOR-ab) with blocking peptide eliminated immunostaining (Negative picture), confirming the specificity of EPOR immunoreactivity. Because EPO is known to stimulate three common cell signal pathways, namely PI3K/Akt, ERK1/2 MAPK and Jak-STAT in cardiomyocytes (Parsa *et al.* 2003), we then assessed ERK and Akt activation (via phosphorylation) in the EPO-treated H9c2 cells in the presence or absence of antibody. Neither EPO nor combined treatment of EPO and antibody affected cell morphology or viability by LDH (Fig. 6B). EPO significantly increased Akt and ERK activity (2.2-fold and 2.1-fold over control, respectively; $P < 0.05$). However, antibody treatment dose-dependently decreased Akt activity and totally abolished ERK activity induced by EPO (Fig. 6C).

EPOR antibody abolishes HPC-mediated changes

The above results indicate the availability of EPOR antibody for neutralizing the biological effect of EPO *in vitro*. We therefore used an EPOR antibody to specifically block EPO signalling in HPC *in vivo*. The post-HPC elevated haematocrit gradually returned to its pre-induction (week 0) level at week 5 and 6 after antibody intervention (Fig. 7A). Antibody treatment of HPC + IR hearts decreased LVDP and increased infarction and plasma CK-MB levels compared to untreated HPC + IR hearts, suggesting that EPOR function is necessary for HPC-mediated protection in IR hearts (Fig. 7B). The antibody significantly reduced mRNA expressions of CXCR4 and CD34 in HPC + IR hearts compared to untreated hearts (Fig. 7C and D), and also reduced SDF-1 expression in HPC + IR hearts (Fig. 7E). The number of CD34⁺ and CXCR4⁺ cells in the HPC + IR blood was 254.6 ± 24.2 and 196.0 ± 20.3 cells per 10⁵ leukocytes, respectively; both were significantly reduced by EPOR antibody, to 119.8 ± 13.2 and 88.7 ± 11.9 cells per 10⁵ leukocytes, respectively ($n = 4$). The total leukocyte count was similar in both blood samples.

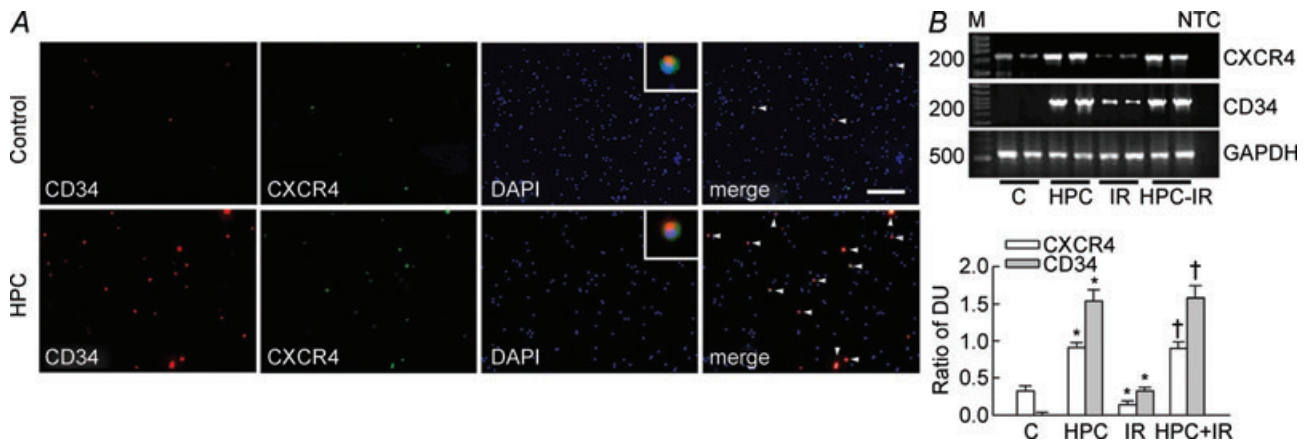


Figure 4. CD34 and CXCR4 expression in the peripheral blood cells and in hearts

A, representative pictures showing the CD34 (red), CXCR4 (green), and nucleus (DAPI, blue) staining in peripheral blood obtained from one control and one HPC rat. The colocalization signal is indicated by arrowheads in the merged picture. Magnification at 100 \times . The inset pictures in the DAPI image show the colocalization of CD34, CXCR4, and nucleus at high magnification. Horizontal bar = 100 μ m. B, the upper panel shows representative blots for the mRNA expression of CXCR4 (224 bases), CD34 (492 bases), and GAPDH (535 bases) ($n = 2$ for each group). Lower bar graph shows the ratio of the DUs for CXCR4 and CD34 compared with GAPDH, respectively ($n = 5$ for each). M, 100 bp DNA ladder. NTC, 'no template control' indicates that the primers were replaced by diethylpyrocarbonate water during PCR. * $P < 0.05$ compared to the control group. † $P < 0.05$ compared to the IR group.

Discussion

Here we demonstrated for the first time that EPO-mediated progenitor cell mobilization was associated in the protection of chronic intermittent hypoxia-exposed hearts. Increased levels of circulating CD34⁺CXCR4⁺ cells and myocardial expression of SDF-1 accompanied

the HPC-mediated reduction of myocardial infarction. These effects were mediated by EPO, since treatment with an antibody against EPOR markedly blocked these effects (Fig. 8). There is no denying that progenitor cell mobilization seen in this study may be one of the phenomena in HPC and is possibly unrelated to HPC-mediated protection against myocardial injury.

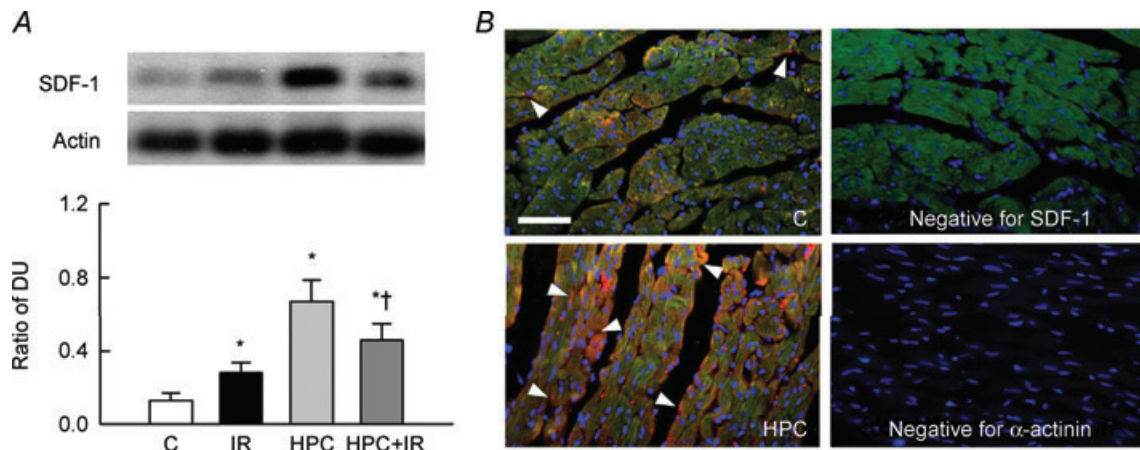


Figure 5. HPC increases SDF-1 expression in hearts

A, representative blots in the upper panel show SDF-1 and actin expression. Lower bar graph shows the ratio of the DUs of SDF-1 and actin for $n = 5$. * $P < 0.05$ compared to the control (C) group. † $P < 0.05$ compared to the IR group. B, representative figures showing SDF-1 expression (red) in the control and HPC hearts at 400 \times magnification. The tissue sections were double stained with α -actinin (green). SDF-1 or α -actinin antibody replaced with a rabbit anti-mouse or anti-goat IgG, respectively, served as a negative control (Negative pictures). Nuclei were counterstained with DAPI (blue). Horizontal bar = 100 μ m.

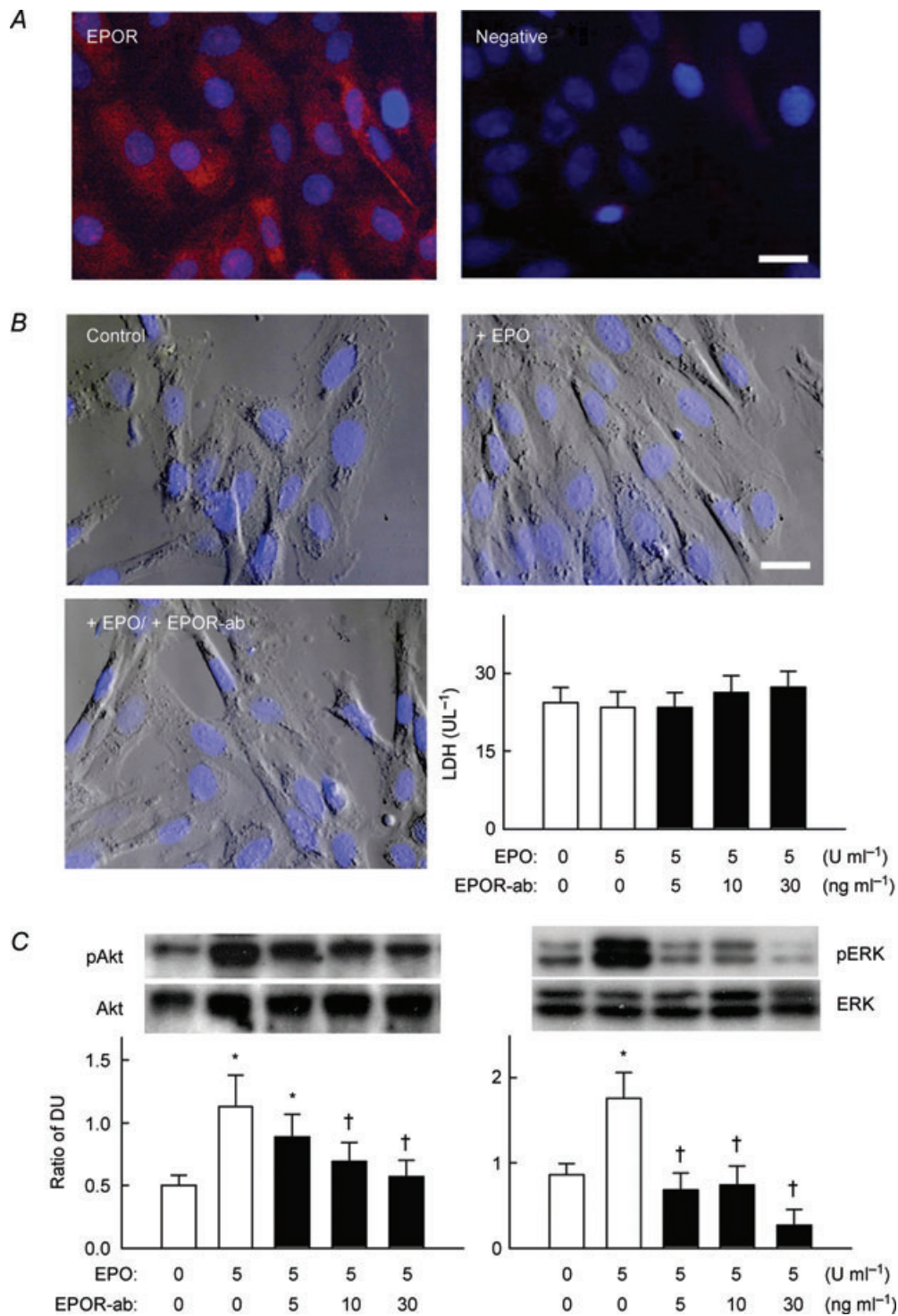


Figure 6. Inhibition of EPO receptor (EPOR) in H9c2 myoblasts

A, left, representative micrograph showing that EPOR was expressed in H9c2 cells. Right, negative picture shows the specificity of EPOR immunoreactivity demonstrated by preadsorption of EPOR antibody with blocking peptide. B, representative micrographs showing cell morphology by phase-contrast in control (untreated) cells, cells treated with 5 U ml⁻¹ of EPO (+EPO), or combination with 5 U ml⁻¹ of EPO and 30 ng ml⁻¹ of EPOR antibody (+EPO/+EPOR-ab) at 400 \times magnification. Nuclei were counterstained with DAPI (blue). Horizontal bar = 10 μ m. Bar graph shows cell viability in different treatments by LDH. C, representative blots in the upper panel showing pAkt, Akt (left), pERK, and ERK (right) expression. Lower bar graph shows the ratio of DU of phosphorylated and total protein for $n = 4$. * $P < 0.05$ compared to the untreated group. † $P < 0.05$ compared to the EPO-treated group.

The dose of antibody given *in vivo* is approximately similar to that tested in the *in vitro* culture system at $\sim 30 \text{ ng ml}^{-1}$. At this dose, both Akt and ERK activation by EPO were totally abolished, and were also significantly reduced when antibody was given at lower doses (Fig. 6), indicating that the antibody is indeed working specifically as a neutralizing antibody.

The repeated hypoxic episodes interspersed with normoxia used in this study is termed chronic intermittent HPC (Neubauer, 2001). This model has been widely used to study the role of HPC in cardiovascular, respiratory and metabolic adaptations (Neubauer 2001). The main feature of HPC that was apparent in the present study was an increased haematocrit (Fig. 1A). Although long-term HPC is known to have detrimental effects on the

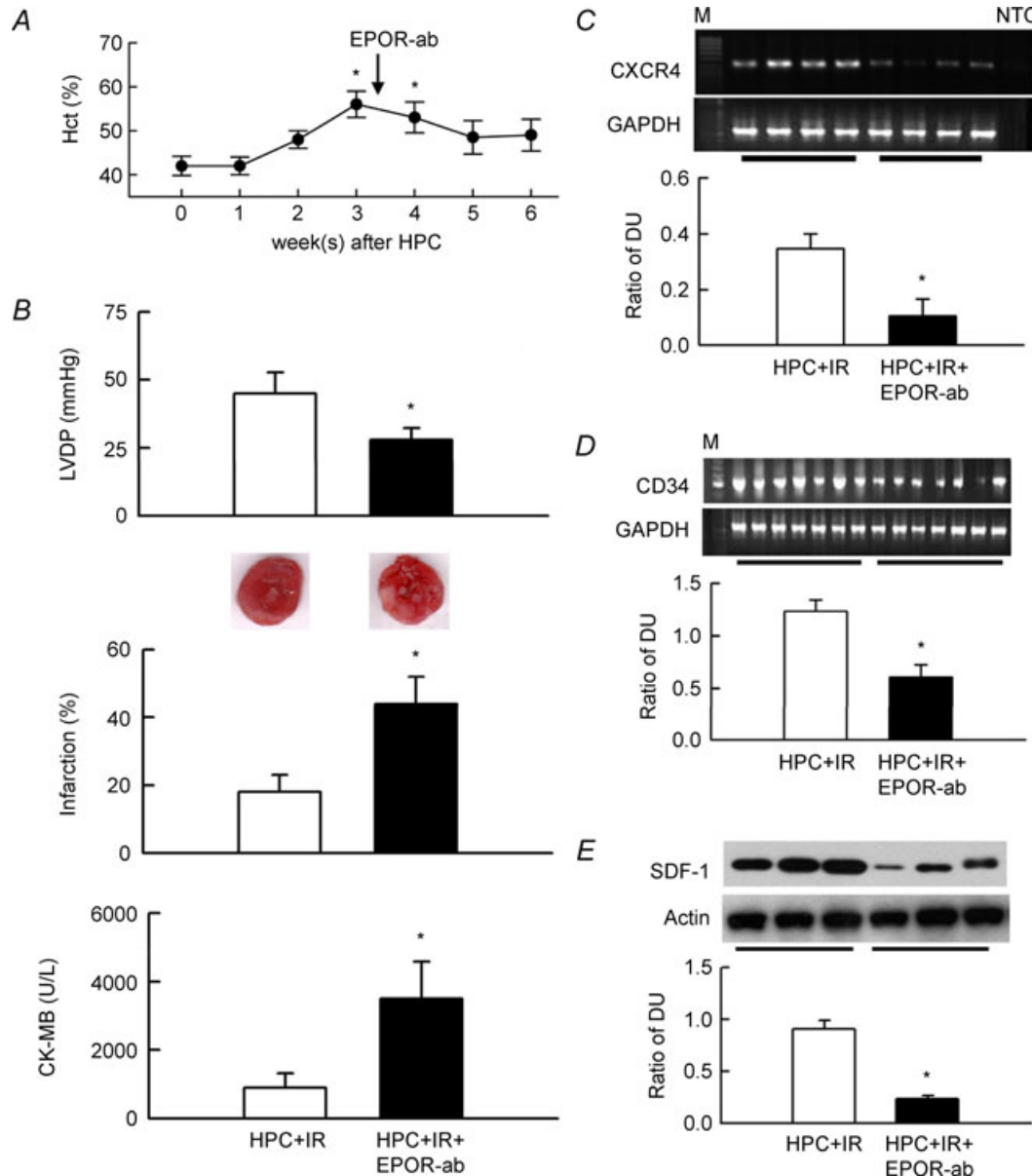


Figure 7. EPO receptor antibody (EPOR-ab) abolishes HPC-mediated functional protection in IR hearts
 A, EPOR-ab given 3 weeks (indicated by arrow) after HPC reduced the haematocrit. * $P < 0.05$ compared to week 0, i.e. before HPC induction. B, changes in LVDP, infarction with representative TTC-stained cardiac sections, and plasma CK-MB in untreated HPC + IR hearts or in hearts treated with EPOR-ab ($n = 7$ for each). * $P < 0.05$ compared to the HPC + IR group. C–E, upper representative blots showing CXCR4 mRNA, CD34 mRNA and SDF-1 protein expressions in 4, 7 and 3 hearts of each group, respectively. Lower bar graph shows the ratio of the DUs for CXCR4 and CD34 to GAPDH ($n = 7$ for each) and SDF-1 to actin ($n = 6$). M, 100 bp of DNA ladder. NTC, no template control. * $P < 0.05$ compared to the HPC + IR group.

cardiovascular system, leading to hypertension and vascular problems (Prabhakar, 2001), our present results indicated that HPC protected hearts against IR injury (Fig. 2). This is consistent with previous studies in hearts that used similar hypoxic episodes to study cardioprotection (Dong *et al.* 2003; Zhu *et al.* 2006; Yeung *et al.* 2007). Repeated reduction of tissue oxygenation during HPC stabilizes the α subunit of the transcription factor HIF-1 (Semenza, 2000). As a result, a number of hypoxia-responsive genes are induced, and two important targets in this process are EPO and VEGF (Maloyan *et al.* 2005). Our results were consistent with these findings, as we observed the elevation of EPO or VEGF in plasma or in cardiac tissues (Figs 1 and 3).

Although we did not study the role of HIF-1 α in HPC-mediated cardioprotection, a study in mice that lack an allele at the *Hif1a* locus showed that EPO mRNA expression in the kidneys is not induced by intermittent hypoxia, and that this mutation abrogates the consequent cardioprotection (Cai *et al.* 2003). Here, blocking EPO function through EPOR antibody completely abolished HPC-mediated protection, thereby demonstrating the importance of EPO in this process (Fig. 7). Highly sensitive mRNA detection methods have previously revealed that EPO mRNA is expressed in heart (Fandrey, 2004). Other studies have also suggested that EPO may be necessary for proper cardiac morphogenesis (Wu *et al.* 1999). No study to date has clearly shown whether intracardial EPO mRNA affects EPO protein synthesis or cardiac function, although bone marrow-expressed EPO appears to be involved in autocrine or paracrine regulation of erythropoiesis (Fandrey, 2004). In the present study, cardiac EPO levels

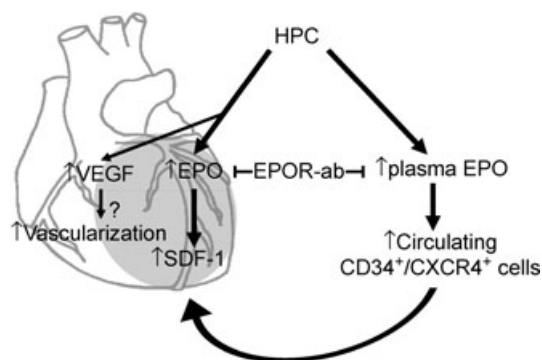


Figure 8. Schematic diagram showing how HPC protects the heart against IR injury

VEGF increased by HPC probably contributes to cardiac neovascularization in early induction. Cardiac EPO and plasma EPO levels are persistently increased by HPC, following which EPO increases SDF-1 expression in the infarct heart (grey area) and also increases circulating CXCR4⁺/CD34⁺ cells to subsequently mobilize to the injury heart. The effect of increased EPO in HPC rats could be specifically blocked by administration of EPO receptor antibody (EPOR-ab).

were markedly increased by HPC, strongly supporting the notion that EPO may act by an autocrine/paracrine mechanism to protect hearts against IR. However, since EPO was also increased in circulation, we cannot rule out the possibility that EPO in the heart was derived from plasma, thereby protecting the heart via an endocrine mechanism (Fig. 1). Previous studies have also questioned whether EPO from the heart itself can protect the myocardium from IR injury, as can be achieved by systemic EPO (Cai *et al.* 2003). Additional studies are therefore required to clarify this.

Unlike the persistent elevation of EPO in hearts, our results showed that VEGF only increased at 1-week HPC and then gradually returned to the control level (Fig. 1C). This is consistent with previous findings of Partovian *et al.* (1998), who showed that there is a 5-fold increase in VEGF mRNA in left ventricle after rats were exposed to 11% oxygen for 1 day, but a prolonged exposure returned its level to baseline. These results imply that the expression of the cardiac VEGF gene is rather insensitive to chronic hypoxia when compared to the EPO gene. But, the increased VEGF at early induction of HPC still plays an important role for cardiac adaptation in HPC since VEGF increase has been shown to be well correlated with neovascularization in hearts (Westenbrink *et al.* 2007). Here we showed that the VEGF level was increased in IR hearts but was unchanged in HPC + IR hearts (Fig. 3). This is contrary to the findings of Westenbrink *et al.* (2007), who showed that EPO treatment increased VEGF expression after myocardial infarction of 9 weeks. Different sources of EPO increase, the level of oxygen tension, and the degree of myocardial injury may probably account for the discrepancy in VEGF induction. However, we speculate that transient severe ischaemia is a potent stimulus for VEGF induction or makes cardiomyocytes more susceptible to exogenous EPO treatment rather than chronic mild hypoxia.

HPC up-regulated SDF-1 more than IR did (Fig. 5A). This could be explained by the different effects of chronic mild hypoxia and transient severe ischaemia on SDF-1 expression. However, the possibility that cardiomyocyte loss during IR affected SDF-1 expression cannot be ruled out, since SDF-1 expression in HPC + IR hearts was lower than that in HPC hearts (Fig. 5). The effect of HPC on SDF-1 depended on the EPO system, as EPOR antibody blocked SDF-1 up-regulation (Fig. 7). Although our study did not examine the mechanisms by which EPO increased SDF-1, studies have shown that cytokines or growth factors target SDF-1 to orchestrate the stem cell-driven repair process (Vandervelde *et al.* 2005). As a cytokine or growth factor, EPO may therefore affect SDF-1 expression directly. This observation is consistent with a previous study showing that EPO induces SDF-1 release from platelets and contributes to ischaemic limb neovascularization (Jin *et al.* 2006). Moreover, SDF-1

induced by VEGF was seen in the formation of angiogenic vessels during wound healing (Grunewald *et al.* 2006) and SDF-1 treatment up-regulated VEGF in the postischaemic hearts (Saxena *et al.* 2008). Further studies are required to clarify the relationship between SDF-1 and VEGF in HPC.

Interestingly, SDF-1 induction in ischaemic tissues has been shown to be directly proportional to the reduction in oxygen tension *in vivo* (Schioppa *et al.* 2003). The mean oxygen tension in the human bone marrow is ~52 mmHg, compared to 85–105 mmHg in the arterial blood (Ishikawa & Ito, 1988), indicating that the bone marrow niche is hypoxic. This suggests that hypoxia-regulated SDF-1 function is a fundamental requirement for progenitor cell trafficking (Kumar *et al.* 2004; Burger & Kipps, 2006). The HPC applied here may have created a conditional environment in hearts that enhanced the recruitment and retention of circulating progenitor cells through SDF-1 function. Though it is unknown whether SDF-1 up-regulation in HPC hearts is tissue-specific, as a stress signal SDF-1 efficiently circles and amplifies the low oxygen environment of postinjury cardiomyocytes and helps sensing of the damaged tissue by circulating stem cells (Abbott *et al.* 2004). Consistent with this notion, IR increased SDF-1 in the infarct tissue and mobilized CD34⁺ cells (Figs 4 and 5). But the recruited cells showed low CXCR4 expression in the IR hearts (Fig. 4), which probably limited the anchoring of these CD34⁺ cells to the injured heart together with low SDF-1 expression. However, HPC largely increased circulating cells expressed with both CD34 and CXCR4 in HPC + IR heart (Fig. 4). Up-regulation of cardiac SDF-1 expression by transplantation of SDF-1-overexpressing fibroblasts or by viral infection can increase stem cell infiltration (Askari *et al.* 2003; Abbott *et al.* 2004). Protection of the postischaemic heart by HPC therefore predominantly relies on the enhanced function of SDF-1 and consequent recruitment of progenitor cells.

Another explanation for the SDF-1 up-regulation shown in Fig. 5 is reduced SDF-1 catabolism in HPC-treated hearts. Proteolytic cleavage is associated with SDF-1 inactivation, as has been demonstrated by several degrading enzymes (Petit *et al.* 2002), including the matrix metalloproteinases (MMP)-2 and MMP-9 that cleave the N-terminus of SDF-1 (McQuibban *et al.* 2001). Interestingly, a previous study by our laboratory showed that EPO prevents IR-mediated increased expression of MMP-2 and MMP-9 in the isolated perfused heart model through ERK activation (Chan *et al.* 2007). It is therefore reasonable to speculate that HPC may promote SDF-1-induced cell chemotaxis in the extracellular matrix component, a process that is disrupted in IR injury by enhanced MMP-2 and MMP-9 levels. Inhibition of EPOR function by specific antibodies also attenuates the HPC-preserved SDF-1 expression in IR hearts (Fig. 7).

Transcripts of CXCR4 but not CD34 were found in control hearts, consistent with previous results showing that CXCR4 is present at the plasmalemma of rat cardiomyocytes (Segret *et al.* 2007). Without CD34, CXCR4 expression in the normal heart probably plays a role in calcium homeostasis regulation, as was previous suggested (Segret *et al.* 2007). Our results show that rats exposed to HPC had increased numbers of circulating CD34⁺CXCR4⁺ cells (Fig. 4). This was consistent with the notion that reducing oxygen tension to 5% augments the production of erythroid, megakaryocytic and granulocytic-monocytic cells in bone marrow stroma (Kumar *et al.* 2004). In different cell types, Schioppa *et al.* (2003) have shown that 1% oxygen largely up-regulates the surface expression of CXCR4, which is sustained for several hours after reoxygenation. They also showed that HIF-1 α interacts with the CXCR4 promoter and increases its mRNA expression, although this was not seen in HIF-1 α knockout mouse embryo fibroblasts (Schioppa *et al.* 2003). Because enhanced HIF-1 α function is known to participate in HPC-mediated adaptations (Neubauer, 2001), we speculated that HIF-1 α may target to CXCR4 during HPC, directly regulating CXCR4 expression. Besides HIF-1 α , CXCR4 expression in various cells and tissues can be attenuated by IL-4 and IL-5 and up-regulated by stem cell factor, IFN- γ , growth factors and steroids (Salcedo *et al.* 2003; Shi *et al.* 2007). In this study, EPO exerted the same stimulating effects on CXCR4 expression, since blockade of EPO function by antibody reduced the homing of CD34⁺CXCR4⁺ cells into injured hearts and subsequently impaired their functional recovery (Fig. 7). However, further studies are required to elucidate the precise effect of EPO on regulating CXCR4. Though the present study offers no data regarding how the SDF-1/CXCR4 axis affects myocardial recovery, previous studies have shown that bone marrow-derived CD34⁺CXCR4⁺ cells act as smooth muscle or endothelial progenitor cells in ischaemic tissue for neointimal formation after vascular injury (Kucia *et al.* 2005a). Consistent with the recent findings, studies have shown that EPO induced improvement of cardiac function in the models of doxorubicin-induced cardiomyopathy, and chronic heart failure mostly relied on the increased mobilization of endothelial progenitor cells (Hamed *et al.* 2006; Westenbrink *et al.* 2007).

In conclusion, the present study demonstrates a crucial role of EPO-regulated SDF-1 expression in the mobilization and possible incorporation of CD34⁺CXCR4⁺ cells into the infarct myocardium in HPC. The therapeutic potential of EPO has been noted in a variety of cardiovascular disorders including myocardial IR (Maiese *et al.* 2005); thus, these results broaden the therapeutic value for clinical application of EPO in the treatment of cardiac diseases.

References

- Abbott JD, Huang Y, Liu D, Hickey R, Krause DS & Giordano FJ (2004). Stromal cell-derived factor-1 α plays a critical role in stem cell recruitment to the heart after myocardial infarction but is not sufficient to induce homing in the absence of injury. *Circulation* **110**, 3300–3305.
- Askari AT, Unzek S, Popovic ZB, Goldman CK, Forudi F, Kiedrowski M, Rovner A, Ellis SG, Thomas JD, DiCorleto PE, Topol EJ & Penn MS (2003). Effect of stromal-cell-derived factor 1 on stem-cell homing and tissue regeneration in ischaemic cardiomyopathy. *Lancet* **362**, 697–703.
- Balsam LB, Wagers AJ, Christensen JL, Kofidis T, Weissman IL & Robbins RC (2004). Haematopoietic stem cells adopt mature haematopoietic fates in ischaemic myocardium. *Nature* **428**, 668–673.
- Bernhardt WM, Warnecke C, Willam C, Tanaka T, Wiesener MS & Eckardt KU (2007). Organ protection by hypoxia and hypoxia-inducible factors. *Methods Enzymol* **435**, 221–245.
- Burger JA & Kipps TJ (2006). CXCR4: a key receptor in the crosstalk between tumor cells and their microenvironment. *Blood* **107**, 1761–1767.
- Cai Z, Manalo DJ, Wei G, Rodriguez ER, Fox-Talbot K, Lu H, Zweier JL & Semenza GL (2003). Hearts from rodents exposed to intermittent hypoxia or erythropoietin are protected against ischemia-reperfusion injury. *Circulation* **108**, 79–85.
- Chan CY, Chen YS, Lee HH, Huang HS, Lai YL, Chen CF & Ma MC (2007). Erythropoietin protects post-ischemic hearts by preventing extracellular matrix degradation: Role of Jak2-ERK pathway. *Life Sci* **81**, 717–723.
- Chen YS, Chien CT, Ma MC, Tseng YZ, Lin FY, Wang SS & Chen CF (2005). Protection 'outside the box' (skeletal remote preconditioning) in rat model is triggered by free radical pathway. *J Surg Res* **126**, 92–101.
- Clanton TL & Klawitter PF (2001). Adaptive responses of skeletal muscle to intermittent hypoxia: the known and the unknown. *J Appl Physiol* **90**, 2476–2487.
- Das DK & Maulik N (2006). Cardiac genomic response following preconditioning stimulus. *Cardiovasc Res* **70**, 254–263.
- Dong JW, Zhu HF, Zhu WZ, Ding HL, Ma TM & Zhou ZN (2003). Intermittent hypoxia attenuates ischemia/reperfusion induced apoptosis in cardiac myocytes via regulating Bcl-2/Bax expression. *Cell Res* **13**, 385–391.
- Fandrey J (2004). Oxygen-dependent and tissue-specific regulation of erythropoietin gene expression. *Am J Physiol Regul Integr Comp Physiol* **286**, R977–R988.
- Feng NH, Lee HH, Shiang JC & Ma MC (2008). Transient receptor potential vanilloid type 1 channels act as mechanoreceptors and cause substance P release and sensory activation in rat kidneys. *Am J Physiol Renal Physiol* **294**, F316–F325.
- Grunewald M, Avraham I, Dor Y, Bachar-Lustig E, Itin A, Jung S, Chimenti S, Landsman L, Abramovitch R & Keshet E (2006). VEGF-induced adult neovascularization: recruitment, retention, and role of accessory cells. *Cell* **124**, 175–189.
- Hamed S, Barshack I, Luboshits G, Wexler D, Deutsch V, Keren G & George J (2006). Erythropoietin improves myocardial performance in doxorubicin-induced cardiomyopathy. *Eur Heart J* **27**, 1876–1883.
- Ishikawa Y & Ito T (1988). Kinetics of hemopoietic stem cells in a hypoxic culture. *Eur J Haematol* **40**, 126–129.
- Jackson KA, Majka SM, Wang H, Pocius J, Hartley CJ, Majesky MW, Entman ML, Michael LH, Hirschi KK & Goodell MA (2001). Regeneration of ischemic cardiac muscle and vascular endothelium by adult stem cells. *J Clin Invest* **107**, 1395–1402.
- Jin DK, Shido K, Kopp HG, Petit I, Shmelkov SV, Young LM, Hooper AT, Amano H, AVECILLA ST, Heissig B, Hattori K, Zhang F, Hicklin DJ, Wu Y, Zhu Z, Dunn A, Salari H, Werb Z, Hackett NR, Crystal RG, Lyden D & Rafii S (2006). Cytokine-mediated deployment of SDF-1 induces revascularization through recruitment of CXCR4⁺ hemangiocytes. *Nat Med* **12**, 557–567.
- Jones SS, D'Andrea AD, Haines LL & Wong GG (1990). Human erythropoietin receptor: cloning, expression, and biologic characterization. *Blood* **76**, 31–35.
- Kolár F, Jezková J, Balková P, Breh J, Neckár J, Novák F, Nováková O, Tomášová H, Srbová M, Ost'ádal B, Wilhelm J & Herget J (2007). Role of oxidative stress in PKC- δ upregulation and cardioprotection induced by chronic intermittent hypoxia. *Am J Physiol Heart Circ Physiol* **292**, H224–H230.
- Kolár F & Ost'ádal B (2004). Molecular mechanisms of cardiac protection by adaptation to chronic hypoxia. *Physiol Res* **53**, S3–S13.
- Kucia M, Ratajczak J & Ratajczak MZ (2005a). Bone marrow as a source of circulating CXCR4⁺ tissue-committed stem cells. *Biol Cell* **97**, 133–146.
- Kucia M, Reza R, Jala VR, Dawn B, Ratajczak J & Ratajczak MZ (2005b). Bone marrow as a home of heterogeneous populations of nonhematopoietic stem cells. *Leukemia* **19**, 1118–1127.
- Kumar R, Stepanek F & Mantalaris A (2004). An oxygen transport model for human bone marrow microcirculation. *Food Bioprocess Process* **82**, 105–116.
- Lachmanova V, Hnilickova O, Povysilova V, Hampl V & Herget J (2005). N-acetylcysteine inhibits hypoxic pulmonary hypertension most effectively in the initial phase of chronic hypoxia. *Life Sci* **77**, 175–182.
- Ma MC, Qian H, Ghassemi F, Zhao P & Xia Y (2005). Oxygen sensitive δ -opioid receptor-regulated survival and death signals: Novel insights into neuronal preconditioning and protection. *J Biol Chem* **280**, 16208–16218.
- Maiese K, Li F & Chong ZZ (2005). New avenues of exploration for erythropoietin. *JAMA* **293**, 90–95.
- Maloyan A, Eli-Berchoer L, Semenza GL, Gerstenblith G, Stern MD & Horowitz M (2005). HIF-1 α -targeted pathways are activated by heat acclimation and contribute to acclimation-ischemic cross-tolerance in the heart. *Physiol Genomics* **23**, 79–88.
- McQuibban GA, Butler GS, Gong JH, Bendall L, Power C, Clark-Lewis I & Overall CM (2001). Matrix metalloproteinase activity inactivates the CXC chemokine stromal cell-derived factor-1. *J Biol Chem* **276**, 43503–43508.

- Milano G, Corno AF, Lippa S, Von Segesser LK & Samaja M (2002). Chronic and intermittent hypoxia induce different degrees of myocardial tolerance to hypoxia-induced dysfunction. *Exp Biol Med (Maywood)* **227**, 389–397.
- Murry CE, Jennings RB & Reimer KA (1986). Preconditioning with ischemia: a delay of lethal cell injury in ischemic myocardium. *Circulation* **74**, 1124–1136.
- Murry CE, Soonpaa MH, Reinecke H, Nakajima H, Nakajima HO, Rubart M, Pasumarthi KB, Virag JJ, Bartelmez SH, Poppa V, Bradford G, Dowell JD, Williams DA & Field LJ (2004). Haematopoietic stem cells do not transdifferentiate into cardiac myocytes in myocardial infarcts. *Nature* **428**, 664–668.
- National Research Council (1996). *Guide for the Care and Use of Laboratory Animals*. National Academy Press, Washington, DC.
- Neubauer JA (2001). Physiological and pathophysiological responses to intermittent hypoxia. *J Appl Physiol* **90**, 1593–1599.
- Parsa CJ, Matsumoto A, Kim J, Riel RU, Pascal LS, Walton GB, Thompson RB, Petrofski JA, Annex BH, Stamler JS & Koch WJ (2003). A novel protective effect of erythropoietin in the infarcted heart. *J Clin Invest* **112**, 999–1007.
- Partovian C, Adnot S, Eddahibi S, Teiger E, Levame M, Dreyfus P, Raffestin B & Frelin C (1998). Heart and lung VEGF mRNA expression in rats with monocrotaline- or hypoxia-induced pulmonary hypertension. *Am J Physiol Heart Circ Physiol* **275**, H1948–H1956.
- Petit I, Szyper-Kravitz M, Nagler A, Lahav M, Peled A, Habler L, Ponomaryov T, Taichman RS, Arenzana-Seisdedos F, Fujii N, Sandbank J, Zipori D & Lapidot T (2002). G-CSF induces stem cell mobilization by decreasing bone marrow SDF-1 and up-regulating CXCR4. *Nat Immunol* **3**, 687–694.
- Prabhakar NR (2001). Oxygen sensing during intermittent hypoxia: cellular and molecular mechanisms. *J Appl Physiol* **90**, 1986–1994.
- Salcedo R, Zhang X, Young HA, Michael N, Wasserman K, Ma WH, Martins-Green M, Murphy WJ & Oppenheim JJ (2003). Angiogenic effects of prostaglandin E2 are mediated by up-regulation of CXCR4 on human microvascular endothelial cells. *Blood* **102**, 1966–1977.
- Saxena A, Fish JE, White MD, Yu S, Smyth JW, Shaw RM, DiMaio JM & Srivastava D (2008). Stromal cell-derived factor-1 α is cardioprotective after myocardial infarction. *Circulation* **117**, 2224–2231.
- Schioppa T, Uranchimeg B, Saccani A, Biswas SK, Doni A, Rapisarda A, Bernasconi S, Saccani S, Nebuloni M, Vago L, Mantovani A, Melillo G & Sica A (2003). Regulation of the chemokine receptor CXCR4 by hypoxia. *J Exp Med* **198**, 1391–1402.
- Segret A, R ucker-Martin C, Pavoine C, Flavigny J, Deroubaix E, Ch atel MA, Lombet A & Renaud JF (2007). Structural localization and expression of CXCL12 and CXCR4 in rat heart and isolated cardiac myocytes. *J Histochem Cytochem* **55**, 141–150.
- Semenza GL (2000). HIF-1: mediator of physiological and pathophysiological responses to hypoxia. *J Appl Physiol* **88**, 1474–1480.
- Shi M, Li J, Liao L, Chen B, Li B, Chen L, Jia H & Zhao RC (2007). Regulation of CXCR4 expression in human mesenchymal stem cells by cytokine treatment: role in homing efficiency in NOD/SCID mice. *Haematologica* **92**, 897–904.
- Tang YL, Qian K, Zhang YC, Shen L & Phillips MI (2005). Mobilizing of haematopoietic stem cells to ischemic myocardium by plasmid mediated stromal-cell-derived factor-1 α (SDF-1 α) treatment. *Regul Pept* **125**, 1–8.
- Vandervelde S, van Luyn MJ, Tio RA & Harmsen MC (2005). Signaling factors in stem cell-mediated repair of infarcted myocardium. *J Mol Cell Cardiol* **39**, 363–376.
- Westenbrink BD, Lipsic E, Van Der Meer P, Van Der Harst P, Oeseburg H, Du Marchie Sarvaas GJ, Koster J, Voors AA, van Veldhuisen DJ, van Gilst WH & Schoemaker RG (2007). Erythropoietin improves cardiac function through endothelial progenitor cell and vascular endothelial growth factor mediated neovascularization. *Eur Heart J* **28**, 2018–2027.
- Wu H, Lee SH, Gao J, Liu X & Iruela-Arispe ML (1999). Inactivation of erythropoietin leads to defects in cardiac morphogenesis. *Development* **126**, 3597–3605.
- Yeung HM, Kravtsov GM, Ng KM, Wong TM & Fung ML (2007). Chronic intermittent hypoxia alters Ca²⁺ handling in rat cardiomyocytes by augmented Na⁺/Ca²⁺ exchange and ryanodine receptor activities in ischemia-reperfusion. *Am J Physiol Cell Physiol* **292**, C2046–C2056.
- Zhu WZ, Xie Y, Chen L, Yang HT & Zhou ZN (2006). Intermittent high altitude hypoxia inhibits opening of mitochondrial permeability transition pores against reperfusion injury. *J Mol Cell Cardiol* **40**, 96–106.

Acknowledgements

This work was supported by grants from the Tao-Yuan General Hospital (TYGH-STU-95B-1 to J.S.L. and M.C.M.) and the Fu Jen Catholic University 10963103990-4 to H.S.C. and M.C.M.